

Can Gamma-Ray Bursts Be Used to Measure Cosmology? A Further Analysis

D. Xu¹, Z. G. Dai¹, and E. W. Liang^{1,2,3}

¹*Department of Astronomy, Nanjing University, Nanjing 210093, China*

²*Department of Physics, Guangxi University, Nanning 530004, China*

³*Department of Physics, University of Nevada, Las Vegas 89154, USA*

ABSTRACT

Two methods of measuring cosmology with gamma-ray bursts (GRBs) have been proposed since a tight relation between the energy of a GRB jet ($E_{\gamma,\text{jet}}$) and its rest frame peak energy of the νF_{ν} spectrum (E'_p), i.e., $(E_{\gamma,\text{jet}}/10^{50}\text{ergs}) = C(E'_p/100\text{keV})^a$, was recently reported, where a and C are dimensionless parameters. A χ^2 statistic technique related with a and C is employed on this issue. In Method I, a and C are recalibrated and then back used in each cosmology. We apply this method to a latest high- z sample of 17 observed GRBs, and obtain the mass density $\Omega_M = 0.16^{+0.46}_{-0.14}$ (1σ) for a flat universe. In Method II, a and C are marginalized in a wide range. For a flat universe, this method gives an improved constraint $\Omega_M = 0.22^{+0.42}_{-0.07}$ (1σ). A combination of SNe Ia and GRBs makes the cosmic concordance model of $\Omega_M = 0.27$ and $\Omega_{\Lambda} = 0.73$ more favored, yielding a $\chi^2_{\text{dof}} = 199.15/172 \approx 1.16$. The SN+GRB sample gives the transition redshift from past deceleration to present acceleration $z_t = 0.64 \pm 0.12$ in the Λ CDM cosmology. In view of the high redshifts for GRBs, we make simulations on the basis of current observations and thus use a large simulated sample to compare the abilities of measuring cosmology with different methods. The results favor that a calibration by low- z bursts (i.e., $z < 0.1$) could not be leaped over mainly because GRBs have not been a standard candle with very low scatter. Future cornucopian observations including the *Swift* satellite are expected to make the *GRB cosmology*, if any, progress from its babyhood into childhood.

Subject headings: gamma rays: bursts — cosmology: observations—cosmology: distance scale

1. Introduction

The traditional cosmology has been revolutionized by modern sophisticated observation techniques in distant Type Ia supernovae (SNe Ia) (e.g., Riess et al. 1998; Schmidt

et al. 1998; Perlmutter et al. 1999; also see Filippenko 2004 for a recent review), cosmic microwave background (CMB) fluctuations (e.g., Bennett et al. 2003; Spergel et al. 2003), and galaxy cluster inventories (e.g., Allen et al. 2003). Modern cosmology has now convincingly suggested that the global mass-energy budget of the universe, and thus its dynamics, is dominated by a dark energy component, and the currently accelerating universe has once been decelerating (e.g., Riess et al. 2004; Tegmark et al. 2004). The cosmography and the nature of dark energy (including its evolution with redshift, if any) are one of the most important issues in physics and astronomy today. Each type of cosmological data trends to play a unique role in measuring cosmology.

Cosmic gamma-ray bursts (GRBs) are the most intense explosions observed so far. They are believed to be detectable up to a very high redshift (Lamb & Reichart 2000; Ciardi & Loeb 2000; Bromm & Loeb 2002), and their high energy photons are almost immune to dust extinction. These advantages would make GRBs an attractive cosmic probe.

From the isotropic-equivalent luminosity ($L_{\gamma,\text{iso}}$) –variability (or spectral lag) relation (Fenimore & Ramirez-Ruiz 2000; Norris, Marani, & Bonnell 2000), a standard energy reservoir of GRBs (Frail et al. 2001), the $L_{\gamma,\text{iso}}-E'_p$ relation (Lloyd-Ronning & Petrosian 2002; Lloyd-Ronning & Ramirez-Ruiz 2002), and the isotropic-equivalent energy ($E_{\gamma,\text{iso}}$)– E'_p relation (Amati et al. 2002) to the beaming-corrected γ -ray energy ($E_{\gamma,\text{jet}}$)– E'_p relation (Ghirlanda, Ghisellini & Lazzati 2004a, GGL relation hereafter), GRBs seem to be towards a more standardizable candle. The two luminosity relations with the variability and spectral lag make GRBs a distance indicator in the same sense as Cepheids and SNe Ia, in which an observed light-curve property can yield an apparent distance modulus (DM). Schaefer (2003) advocated a new method (hereafter Method I) of measuring cosmology with GRBs by considering these two luminosity indicators for nine GRBs with known redshifts, and gave the constraint $\Omega_M < 0.35$ (1σ ; Λ -models) for a flat universe. Similar to the brightness of SNe Ia, the energy reservoirs in GRB jets are also clustered. Bloom et al. (2003) used different standard energy reservoir assumptions but got meaningless constraints because of the large dispersion of $E_{\gamma,\text{jet}}$, which might be caused by the inhomogeneous origin of the bursts. Amati et al. (2002) found the $E_{\gamma,\text{iso}} \propto E'_p^k$ (where $k \sim 2$) relation from 12 *BepoSAX* bursts. Sakamoto et al. (2004a) and Lamb et al. (2004) found the *HETE-2* observations confirm this relation and extend it to X-ray flashes. In addition, it also holds within a GRB (Liang, Dai & Wu 2004). The tight GGL relation, i.e., $(E_{\gamma,\text{jet}}/10^{50}\text{ergs}) = C(E'_p/100\text{keV})^a$, makes GRBs a more standardizable candle. Physical explanations of this relation are involved to the standard synchrotron mechanism in relativistic shocks (Zhang & Mészáros 2002; Dai & Lu 2002) or the emission from off-axis relativistic jets (Yamazaki, Ioka & Nakamura 2004; Eichler & Levinson 2004), together with the afterglow jet model (e.g., Sari et al 1998; Sari et al. 1999). According to these explanations, $a \sim 1.5$ might be intrinsic. Dai, Liang & Xu

(2004, DLX04) proposed a different method (hereafter Method II) for 12 GRBs with known redshifts, and gave the constraint $\Omega_M = 0.35 \pm 0.15$ (1σ) for a flat universe with marginalizing over C and considering $a = 1.5$ being intrinsic. Following Schaefer's method, Ghirlanda et al. (2004b) and Friedman & Bloom (2004) also used the GGL relation to investigate the same issue but obtained some inconsistent results.

Because of the lack of low- z GRBs, Methods I and II are different from the “Classic Hubble Diagram” method in the SNe Ia. High- z GRBs also present complemental contents to the *SN cosmology*. In this paper, our attention is focused on constraining the $\Omega_M - \Omega_\Lambda$ parameters and the transition redshift using the latest 17 GRB sample and the GRB+SN sample (SN data taken from the gold sample in Riess et al. 2004). Thanks to the negative effect of present non-calibration and the positive factor of high redshifts for GRBs, it is necessary to use a large simulated GRB sample to compare the abilities of measuring cosmology with different methods. Our simulations are subject to the current observational accuracy.

This paper is arranged as follows. In section 2, we describe our data and analytical method. The results from the observed GRB sample are presented in section 3. In sections 4, we perform Monte Carlo simulations to compare the ability of constraining cosmology with different methods. Conclusions and discussion are presented in section 5.

2. Data and Methods Analysis

2.1. Sample Analysis

The great diversity in GRB phenomena suggests that the GRB population may consist of substantially different subclasses (e.g. MacFadyen & Woosley 1999; Bloom et al. 2003; Sazonov et al. 2004; Soderberg et al. 2004). To make GRBs a standard candle, a homogenous GRB sample is required. The most prominent observational evidence for a GRB jet is its temporal break in their afterglow light curves. For some bursts, e.g., GRB030329, their temporal breaks are observed in both the optical and radio bands. Berger et al. (2003) argued that these two breaks are caused by the narrow component and wide component of the jet in this burst, respectively, indicating that the physical origins of the breaks in the optical band and in the radio band are different. In addition, the radio afterglow light curves fluctuate significantly. For example, in the case of GRB970508, the light curve of its radio afterglow does not present clearly a break. Only a lower limit of $t_j > 25$ days was proposed by Frail et al. (2000). Furthermore, the light curve of its optical afterglow is proportional to $t^{-1.1}$, in which case no break appears (Galama et al. 1998). We thus include only those bursts that their temporal breaks in optical afterglow light curves were well measured in our

analysis. We obtain a sample of 17 GRBs excluding GRB970508. They are listed in Table 1.

We correct the observed fluence in a given bandpass to a “bolometric” bandpass of 1 – 10^4 keV with spectral fitting parameters. Spectral fittings to observations in different energy bands for one burst may present different results. This difference may significantly affect the bolometric correction. We thus collect the fluence and the spectral fitting parameters from the same original literature as possible. For GRB 970828, GRB 980703, GRB 991216, and GRB 020124, the fluence and the spectral parameters are unavailable from one original literature, so we choose their fluences measured in the widest energy band available in the literature.¹

For GRB 011211, we approximately take the high-energy spectral index β to be -2.3 because it is unreported in Amati (2004). The spectra of *HETE-2*-detected GRB020124, GRB020813, GRB021004, GRB030226 and XRF030429 are not fitted by the Band function but the cutoff power law model. However, it is appropriate that their corresponding “bolometric” fluences are calculated by the former model with $\beta \sim -2.3$, avoiding the potential systematical bias from detecting disability in high-energy bands for the *HETE-2* bursts (Barraud et al. 2003).

The medium densities of several bursts in our sample have been obtained from broad-band modelling of the afterglow emission (e.g., Panaiteescu & Kumar 2002). For the bursts with unknown n , we take $n \simeq 3 \text{ cm}^{-3}$ with an error of 0.3 (Ghirlanda et al. 2004a and references therein).

2.2. Method Analysis

According to the relativistic fireball model, the emission from a spherically expanding shell and from a jet would be rather similar to each other, if the observer is along the jet’s axis and the Lorentz factor of the fireball is larger than the inverse of the jet’s half-opening angle θ ; but when the Lorentz factor drops below θ^{-1} , the jet’s afterglow light curve is expected to present a break because of sideways expansion (Rhoads 1999; Sari, Piran & Halpern 1999). Therefore, together with the assumptions of the initial fireball emitting a constant fraction

¹It should be noted here that we have also corrected some wrong data in Ghirlanda et al. (2004b) and Friedman & Bloom (2004). For example, (i) the peak energy E_p^{obs} of GRB021004 cited by Friedman & Bloom (2004) has been corrected in Sakamoto et al. (2004b), (ii) the E_p^{obs} of GRB020405 should be 192.5 keV (Price et al. 2003) after correctly understanding the reported energy parameter of the Band function as the break energy E_b rather than the characteristic energy E_0 .

η_γ of its kinetic energy into the prompt γ -rays and a constant circum-burst density medium of number density n , the jet's half-opening angle is given by

$$\theta = 0.161 \left(\frac{t_{j,d}}{1+z} \right)^{3/8} \left(\frac{n_0 \eta_\gamma}{E_{\gamma,\text{iso},52}} \right)^{1/8} \quad (1)$$

where $E_{\gamma,\text{iso},52} = E_{\gamma,\text{iso}}/10^{52}$ ergs, $t_{j,d} = t_j/1$ day, $n_0 = n/1$ cm $^{-3}$. The value of η_γ is taken as 0.2 throughout this paper (Frail et al. 2001). The “bolometric” isotropic-equivalent γ -ray energy of a GRB is given by

$$E_{\gamma,\text{iso}} = \frac{4\pi d_L^2 S_\gamma k}{1+z}, \quad (2)$$

where S_γ is the fluence (in units of erg cm $^{-2}$) received in an observed bandpass and the quantity k is a multiplicative correction of order unity relating the observed bandpass to a standard rest-frame bandpass (1-10 4 keV in this paper) (Bloom, Frail & Sari 2001). The energy release of a GRB jet is thus given by

$$E_{\gamma,\text{jet}} = (1 - \cos \theta) E_{\gamma,\text{iso}}. \quad (3)$$

The GGL relation is

$$(E_{\gamma,\text{jet}}/10^{50} \text{ ergs}) = C (E'_p/100 \text{ keV})^a \quad (4)$$

where a and C are dimensionless parameters. Combining equations (1)-(4) and assuming² $\theta \ll 1$, we approximate the apparent luminosity distance of a GRB as

$$d_L = 7.69 \frac{(1+z) C^{2/3} [E_p^{\text{obs}} (1+z)/100 \text{ keV}]^{2a/3}}{(k S_\gamma t_{j,d})^{1/2} (n_0 \eta_\gamma)^{1/6}} \text{ Mpc} \quad (5)$$

with the uncertainty being

$$\begin{aligned} \left(\frac{\sigma_{d_L}}{d_L} \right)^2 &= \left(\frac{\sigma_k}{2k} \right)^2 + \left(\frac{\sigma_{S_\gamma}}{2S_\gamma} \right)^2 + \left(\frac{\sigma_{t_{j,d}}}{2t_{j,d}} \right)^2 + \left(\frac{\sigma_{n_0}}{6n_0} \right)^2 + \left(\frac{2a}{3} \frac{\sigma_{E_p^{\text{obs}}}}{E_p^{\text{obs}}} \right)^2 \\ &+ \left(\frac{2}{3} \frac{\sigma_C}{C} \right)^2 + \left(\frac{2a}{3} \frac{\sigma_a}{a} \ln \frac{E_p^{\text{obs}} (1+z)}{100} \right)^2 \end{aligned} \quad (6)$$

. The apparent DM of a burst can thus be given by

$$\mu_{\text{obs}} = 5 \log d_L + 25 \quad (7)$$

²This assumption is valid because $|(1 - \cos \theta - \theta^2/2)/(1 - \cos \theta)| < 1\%$ when $\theta < 0.35$, and $< 0.4\%$ when $\theta < 0.22$.

with the uncertainty of

$$\sigma_{\mu_{\text{obs}}} = \frac{5}{\ln 10} \frac{\sigma_{d_L}}{d_L}. \quad (8)$$

In the case that the GGL relation is not calibrated by low- z bursts, the χ^2 statistic in Λ CDM models is:

$$\chi^2(\Omega_M, \Omega_\Lambda, a, C | h) = \sum_i \left[\frac{\mu_{\text{th}}(z_i; \Omega_M, \Omega_\Lambda | h) - \mu_{\text{obs}}(z_i; \Omega_M, \Omega_\Lambda, a, C | h)}{\sigma_{\mu_{\text{obs}}(z_i; \Omega_M, \Omega_\Lambda, a, C, \sigma_a/a, \sigma_C/C)}} \right]^2 \quad (9)$$

where the dimensionless Hubble constant $h \equiv H_0/100 \text{ km s}^{-1}\text{Mpc}^{-1}$ is taken as 0.71. If this relation is calibrated, the χ^2 statistic turns to be:

$$\chi^2(\Omega_M, \Omega_\Lambda, h) = \sum_i \left[\frac{\mu_{\text{th},i}(z_i; \Omega_M, \Omega_\Lambda, h) - \mu_{\text{obs},i}}{\sigma_{\mu_{\text{obs},i}}} \right]^2 \quad (10)$$

where h should be marginalized.

3. Cosmological Constraints

The luminosity distance in Λ -models is given by

$$\begin{aligned} d_L &= c(1+z)H_0^{-1}|\Omega_k|^{-1/2} \text{sinn}\{|\Omega_k|^{1/2} \\ &\quad \times \int_0^z dz[(1+z)^2(1+\Omega_M z) - z(2+z)\Omega_\Lambda]^{-1/2}\}, \end{aligned} \quad (11)$$

where $\Omega_k = 1 - \Omega_M - \Omega_\Lambda$, and “sinn” is \sinh for $\Omega_k > 0$ and \sin for $\Omega_k < 0$. For $\Omega_k = 0$, Eq. 10 degenerates to be $c(1+z)H_0^{-1}$ times the integral.

Thanks to unknown a and C , Method I suggests the following procedure to constrain Ω_M and Ω_Λ : (1) a best-fit of the GGL relation for a given i th cosmic model is made to yield a set of $(a, C)_i$ and $(\sigma_a/a, \sigma_C/C)_i$; (2) the $(a, C)_i$ and $(\sigma_a/a, \sigma_C/C)_i$ are used back in the i th model to obtain χ_i^2 ; and (3) confidence contours are plotted according to the likelihood by $P_i \propto e^{-\chi_i^2/2}$. Constraints from 17 GRBs on the $\Omega_M - \Omega_\Lambda$ parameters with this method are shown in Fig 1 (blue contours). The data set is consistent with the cosmic concordance model of $\Omega_M = 0.27$ and $\Omega_\Lambda = 0.73$, yielding a $\chi_{\text{dof}}^2 = 17.74/15 \approx 1.18$. We measure $\Omega_M = 0.16^{+0.42}_{-0.14}$ (1σ) for a flat universe.

DLX04 proposed Method II based on the principle that if there are unknown cosmology-independent parameters in the χ^2 statistic, they are usually marginalized, i.e., integrating the parameters according to their probability distribution. For SNe Ia, the nuisance parameter h is marginalized in a wide range (e.g. Riess et al. 2004), or the slope of the Phillips relation

α and the “Hubble constant-free” B-band peak absolute magnitude \mathcal{M} are integrated (Knop et al. 2003). For GRBs, DLX04 made marginalization to h and C (uniform distribution assumed), treating $a = 1.5$ as intrinsic. In this paper, we give up this scenario for the purpose of universality and suggest an improved procedure for this method as follows: (1) a best-fit of the GGL relation in every cosmic model is made to yield all sets of $(a, C)_j$ and $(\sigma_a/a, \sigma_C/C)_j$ ($j = 1, N$); (2) all sets of $(a, C)_j$ and $(\sigma_a/a, \sigma_C/C)_j$ are used in the i th model to obtain its likelihood of $P_i \propto \sum_j \exp(-\chi_j^2/2)$; and (3) repeat Step 2 from $i = 1$ to $i = N$ to get the likelihood in any cosmic model. Constraints from 17 GRBs on the $\Omega_M - \Omega_\Lambda$ plane with this method are also shown in Fig 1 (red contours), which are improved compared with that from Method I. Method II gives a $\chi_{dof}^2 = 17.65/15 \approx 1.18$ in the $(0.27, 0.73)$ cosmology. We measure $\Omega_M = 0.22_{-0.07}^{+0.42}$ (1σ) for a flat universe.

By Method I, we find the half-opening angles of all the bursts are less than 0.2 rad in the $(0.27, 0.73)$ model and even less than 0.22 rad in any cosmic model.³ The typical σ_a/a and σ_C/C are 5% and 10%. Parameters a and C are in the ranges of $[1.40, 1.68]$ and $[0.70, 1.30]$, respectively. So typical error terms in Eq. 6 are $\sigma_k/2k \sim 0.025$, $\sigma_{S_\gamma}/2S_\gamma \sim 0.050$, $\sigma_{t_{j,d}}/2t_{j,d} \sim 0.098$, $\sigma_{n_0}/6n_0 \sim 0.038$, $(2a/3)(\sigma_{E_p^{obs}}/E_p^{obs}) \sim 0.171$, $(2/3)(\sigma_C/C) \sim 0.067$, and $(2a/3)(\sigma_a/a)(\ln[E_p^{obs}(1+z)/100]) \sim 0.058$. The average uncertainty of apparent DM for GRBs is ~ 0.49 , which is about twice of that in SNe Ia. It means that GRBs need to be developed into a lower-scatter standard candle.

Here we also present how well the 17 GRBs could constrain the $\Omega_M - \Omega_\Lambda$ parameters if the GGL relation was calibrated (*for illustrative purpose only*). The parameters a , C , σ_a/a and σ_C/C are *empirically* taken as 1.5, 1.0, 0.05 and 0.1, respectively.⁴ The results are shown as dashed contours in Fig 1. We get $\Omega_M = 0.18_{-0.02}^{+0.12}$ (1σ) for a flat universe, and a $\chi_{dof}^2 = 18.64/15 \approx 1.24$ for the $(0.27, 0.73)$ model. As can be seen, a low- z calibration would make GRBs place much stringent constraints.

A combination of SNe Ia and GRBs will give new contents on cosmography, although the results are dominated by alone SNe (Method II for GRBs). The results are shown in Fig 2. The SN, SN+GRB data are consistent with the cosmic concordance model of $\Omega_M = 0.27$, respectively yielding $\chi_{dof}^2 = 178.17/155 \approx 1.15$ and $\chi_{dof}^2 = 199.15/(157 + 17 - 2) \approx 1.16$. However, the confidence region at 1σ level moves more near to the $(0.27, 0.73)$ cosmology and thus better consistent with the conclusions from WMAP observations (Spergel et al. 2003).

³ Ω_M and Ω_Λ are taken from 0 to 1.

⁴The parameters a and C are related with the physical origin of GRB phenomena, so future determination of a and C needs theoretical progress in this field, not only observations.

Furthermore, we determine the transition redshift z_t with the SN and SN+GRB data. Usually, two approaches are used on this subject. In the Λ CDM models, z_t is calculated by $z_t = \sqrt[3]{2\Omega_\Lambda/\Omega_M} - 1$. With this approach, the transition redshift derived from the SN and SN+GRB samples changes from $z_t = 0.62 \pm 0.10$ (dashed curves in Fig 3) to $z_t = 0.64 \pm 0.12$ (solid curves in Fig 3). Another approach is to determine the present deceleration factor q_0 and its changing rate at the present epoch q_1 after rewriting the luminosity distance in terms of $q(z) = q(q_0, q_1, z)$ (Riess et al. 2004). The transition redshift is thus obtained at $q(z_t) = 0$. Here we propose a new parameterization as $q(z) = q_0 + q_1 \frac{z}{1+z}$, which is suitable to the low- and high- z objects. With this approach, the SN sample gives $z_t = 0.45 \pm 0.10$ and the SN+GRB sample gives $z_t = 0.54 \pm 0.18$. In both approaches, the addition of high- z GRBs leads to a slightly larger z_t , which is near 0.60.

4. Simulations and Cosmological Ability Tests

4.1. Procedure of Simulations

Detected GRBs are becoming more and more while so far a low- z sample has not been established, a question naturally emerges: can a large GRB sample without low- z bursts effectively measure cosmology? To answer this question, we make a Monte Carlo simulation and thus use a large simulated sample to present a comparison analysis with Method I, II and an assumption of $a = 1.5$ and $C = 1.0$.

Our simulations are based on the GGL relation in the (0.27, 0.73) cosmic model from the GRB sample in Table 1. In this model, we find that $a = 1.512$, $C = 0.990$ ($\chi^2_\nu = 21.75/15 = 1.45$; see Press et al. 1999), $\theta < 0.2$ rad, and $E_{\gamma, \text{jet}} \in [6.38 \times 10^{49}, 8.47 \times 10^{51}]$ ergs. The observed peak energy E_p is of $[35.0, 780.8]$ keV. These restrictive conditions are imposed upon our simulations. Each simulated GRB is characterized by a set of S_b , t_j , n , z and E_p , where S_b is the “bolometric” fluence in gamma-ray band. The simulation procedure is as follows:

(1) We derive the distributions of observational quantities S_b , t_j , n , and z and their uncertainties. It is impossible to establish robust distributions from the current GRB sample. From the 17 GRBs in Table 1, we find $S_b \in [9.10 \times 10^{-7}, 6.08 \times 10^{-4}]$ erg cm $^{-2}$ with $\langle \Delta S_b/S_b \rangle = 0.115 \pm 0.043$, and $t_j \in [0.43, 4.74]$ days with $\langle \Delta t_j/t_j \rangle = 0.196 \pm 0.134$. We thus simply assume that S_b and t_j uniformly distribute in these ranges with Gaussian distributions for their errors. Because n is unavailable in the literature for most GRBs, we take the distribution of n to be a random distribution in $[1, 10]$ cm $^{-3}$ (e.g. Frail et al. 2001; Ghirlanda et al. 2004a) with a Gaussian distribution for $\langle \Delta n/n \rangle = 0.5 \pm 0.2$. The quantity

of z is taken according to the observational distribution with an upper limit $z \sim 4.5$ (Bloom et al. 2003) and its error is ignored. We also get $\langle \Delta E_p/E_p \rangle = 0.171 \pm 0.085$ from the 17 GRBs.

(2) We randomly generate a GRB characterized by a set of $(S_b \pm \Delta S_b, t_j \pm \Delta t_j, n \pm \Delta n$ and $z)$ from the distributions described in (1), compute its $E_{\gamma, \text{jet}}$ in the $(0.27, 0.73)$ model, and then calculate its E_p by the GGL relation of $(1.512, 0.990)$.

(3) The GRB generated in step (2) rigidly follows the GGL relation. We add a random deviation to each parameter to make this burst more realistic, i.e., $S'_b = S_b + 0.8(-1)^m \Delta S_b$, $t'_j = t_j + 0.8(-1)^m \Delta t_j$, and $n' = n + 0.8(-1)^m \Delta n$, where m is randomly taken as 0 and 1. We then calculate θ' and $E'_{\gamma, \text{jet}}$. We also add a random deviation to the E_p value obtained in step 2, i.e., $E'_p = E_p + 0.8(-1)^m \Delta E_p$, where $\Delta E_p/E_p$ is randomly selected according to its Gaussian distribution.

(4) Since $\theta < 0.2$ rad, $E_{\gamma, \text{jet}} \in [6.38 \times 10^{49}, 8.47 \times 10^{51}]$ erg and $E_p \in [35.0, 780.8]$ keV for the 17 GRBs in Table 1, we require θ' , $E'_{\gamma, \text{jet}}$, and E'_p of a simulated GRB have to within these ranges, respectively.

(5) Repeat steps (2)-(4) to generate a sample of 157 bursts.

We find the half-opening angles of the simulated sample are also less than 0.22 rad for various cosmic models as in the observed sample. The $E_{\gamma, \text{jet}}$ as a function of $E_p(1+z)$ is shown in Figure 3: open circles for the simulated GRBs and filled triangles for the observed GRBs.

Please note that the simulated sample is based on the $(0.27, 0.73)$ cosmic model. We carry out a circular operation to compare the abilities of measuring cosmology with different methods for a large high- z sample. This is the aim of our simulations.

4.2. Tests With Different Methods

Joint confidence contours from the simulated sample with Method I are shown in Fig 4 (solid contours). The results with Method II are shown in Fig 5 (solid contours). We see that although more stringent confidence intervals are obtained using a large sample, Method I and II can not make GRBs effectively measure cosmology.

By Method I, we find the average σ_a/a and σ_C/C for the simulated sample decrease to 0.02 and 0.05. The main reason is that, for the small observed sample, the dispersion is mainly contributed by the four “outliers”; while for the large simulated sample, the bursts

are distributed around the “rigid” GGL relation with a Gaussian distribution. Such a large sample seems to be more realistic.

We further make test with the assumption of a , C , σ_a/a and σ_C/C being 1.5, 1.0, 0.02 and 0.05, respectively. The results are shown in Fig 6 (red contours). As can be seen, a low- z calibrated GGL relation would make a large sample with a similar observational accuracy place firm constraints, which are comparable to that from SNe Ia (blue contours). The simulated sample is consistent with its founded cosmic model of $(0.27, 0.73)$, yielding $\chi^2_{dof} = 176.33/155 \approx 1.14$ with Method I, $\chi^2_{dof} = 175.30/155 \approx 1.13$ with Method II, and $\chi^2_{dof} = 175.49/155 \approx 1.13$ with the assumption of $a = 1.5$ and $C = 1.0$. The χ^2 values in the three scenarios are approximately the same, but contour intervals are far different.

The results with Method I and II are mainly affected by three factors: the redshifts of the objects, the number of the objects and scatter of the standard candle. In the Hubble diagram, various cosmic models differ more and more as z increases while degenerate more heavily as z decreases. Thus, Method I and II could effectively measure cosmology for the high- z and low-scatter standard candles. However, we found that even when the redshifts of the simulated bursts, selected according to the cosmic star formation rate, are up to $z \sim 8$ (Prochani & Madau 2001), Method I and II still cannot give firm constraints at a high confidence level. On the other hand, due to current observational conditions, it is difficult for GRBs to be developed into an excellent low-scatter standard candle in the near future. Therefore, we tend to favor that a calibration by low- z bursts could not be leaped over on this issue.

5. Conclusions and Discussion

In the present stage, GRBs with known redshifts are less than 40 out of a few thousands, among which 17 are available to derive the GGL relation. However, none of the 17 bursts owns a low redshift (i.e. $z < 0.1$). So the small sample and non-calibration by low- z bursts make GRBs give rather loose constraints on cosmography. Even so, GRBs independently give the constraints on the mass density $\Omega_M = 0.22^{+0.42}_{-0.07}$ (1σ) for a flat Λ CDM model. Meanwhile, 17 GRBs have added the new contents to the *SN cosmology*: the cosmic concordance model of $\Omega_M = 0.27$ and $\Omega_\Lambda = 0.73$ are more favored; and the transition redshift z_t is slightly lifted but near 0.6.

Similar to the history of SNe Ia, GRBs are brought to a more and more standardized candle. By the GGL relation, the scatter in GRBs have been about twice of that in SNe Ia. Long GRBs are commonly regarded as the products of evolving massive stars, so the same

physical origin would make them within a homogeneous class. In addition, the advantages of high redshifts and immunity to the dust extinction for GRBs make up, to a certain extent, the weakness of current relative large scatter. The dashed confidence contours in Fig 1 indicate how well the 17 GRBs are expected to further narrow down the parameters if this relation is calibrated by low- z bursts. GRBs can observe the deep deceleration phase of the universe up to $z \sim 20$, which would greatly contribute to the constraints on dark energy and its evolution with model-independent experiments (Daly & Djorgovski 2003). Furthermore, the shape of the confidence contours in Fig 7 imply that standard candles whose redshifts are up to a few, of which GRB is an competitive candidate, would not only provide evidence for cosmic acceleration but well constrain the mass density Ω_M . The *Swift* satellite is hopeful to establish a large sample with secure redshifts, perhaps including nearby bursts. In this sense, the *GRB cosmology* now lies in its babyhood.

A reliable physical basis of the GGL relation is critical for GRBs as a cosmic ruler. Using the small jet-angle approximation, simple scaling deduction gives $E_{\gamma, \text{jet}} \propto E'_p^{1.5}$ (or $E'_p \propto E_{\gamma, \text{jet}}^{2/3}$) under the conditions that other physical parameters such as the energy equipartition factor ε_e of the electrons, the energy equipartition factor ε_B of magnetic field, the bulk Lorentz factor Γ , etc., or their combinations are clustered (Zhang & Mészáros 2002; Dai & Lu 2002; Wu, Dai & Liang 2004). However, the explanations of this relation, including the microphysical processes and the origin of long GRBs, need further investigation. Whether $a \sim 1.5$ being intrinsic or not will be tested by future observations of low- z bursts. It should also be pointed out that although the GGL relation seems to be tight enough, it strongly relies on the GRB afterglow jet model and various measurements (about half of the z -known bursts available). New relations, which relate with as few well-observed quantities as possible, are required for improvement.

Addendum: We have noticed that recent works on this issue from Firmani et al. (astro-ph/0501395) and Friedman & Bloom (2004, revised version). Discussions on optimization of the method and decrease of the error of apparent DM for GRBs are presented elsewhere.

XD is grateful to X.L. Luo for helpful discussions. This work was supported by the National Natural Science Foundation of China (grants 10233010, 10221001, and 10463001), the Ministry of Science and Technology of China (NKBRSF G19990754), the National Post Doctoral Foundation of China, and the Research Foundation of Guangxi University.

REFERENCES

Amati, L. et al. 2000, *Science*, 290, 953

Amati, L. et al. 2002, *A&A*, 390, 81

Andersen, M. I. et al. 2003, *GCN*, 1993

Atteia, J. L. 2003, *A&A*, 407, L1

Barraud, C. et al. 2003, *A&A*, 400, 1021

Barth, A. J. et al. 2003, *ApJ*, 584, L47

Band, D.L., Matteson, J., Ford, L., et al. 1993, *ApJ*, 413, 281

Bennett, C. L. et al. 2003, *ApJS*, 148, 1

Berger, E. et al. 2001, *ApJ*, 556, 556

Berger, E. et al. 2003, *Nature*, 426, 154

Bjornsson G. et al. 2001, *ApJ*, 552, L121

Bloom, J. S., Frail, D. A., & Sari, R. 2001, *AJ*, 121, 2879

Bloom, J. S., Frail, D. A., & Kulkarni, S. R. 2003, *ApJ*, 594, 674

Bromm, V., & Loeb, A. 2002, *ApJ*, 575, 111

Ciardi, B., & Loeb, A. 2000, *ApJ*, 540, 687

Crew, G. B. et al. 2003, *ApJ*, 599, 387

Dai, Z. G., & Lu, T. 2002, *ApJ*, 580, 1013

Dai, Z. G., Liang, E. W. & Xu, D. 2004, *ApJ*, 612, L101 (DLX04)

Daly, R. A. & Djorgovski, S. G. 2003, *ApJ*, 597, 9

Djorgovski, S. G. et al. 1998a, *GCN*, 189

Djorgovski, S. G. et al. 1998b, *GCN*, 137

Djorgovski, S. G. et al. 2001, *ApJ*, 526, 654

Eichler, D., & Levinson, A. 2004, preprint (astro-ph/0405014)

Filippenko, A. V. 2004, astro-ph/0410609

Frail, D. A., Waxman, E., and Kulkarni, S. R. 2000, *ApJ*, 537, 191

Frail, D. A. et al. 2001, *ApJ*, 562, L55

Frail, D. A. et al. 2003, *ApJ*, 590, 992

Friedman, A. S. & Bloom, J. S., *astro-ph/0408413*

Fruchter, A. et al. 1999, *ApJ*, 519, L13

Galama, T. J. et al. 1998, *ApJ*, 497, L13

Galama, T. J. et al. 1999, *GCN*, 338

Ghirlanda, G., Ghisellini, G., & Lazzati, D. 2004a, *ApJ*, 616, 331 (GGL)

Ghirlanda, G. et al. 2004b, *ApJ*, 613, L13

Greiner, J. et al. 2002, *GCN*, 1886

Greiner, J. et al. 2003, *GCN*, 2020

Halpern, J. P., et al. 2000, *ApJ*, 543, 697

Hjorth, J. et al. 1999, *GCN*, 219

Hjorth, J. et al. 2003, *ApJ*, 597, 699

Holland, et al. 2002, *AJ*, 124, 639

Holland, et al. 2003, *AJ*, 125, 2291

Holland, et al. 2004, *astro-ph/0405062*

Israel, G. L. et al. 1999, *A&A*, 348, L5

Jakobsson, P. et al. 2003, *A&A*, 408, 941

Jakobsson, P. et al. 2004, *A&A*, 427, 785

Jimenez, R., Band, D. L., & Piran, T., 2001, *ApJ*, 561, 171

Klose, S. et al. 2004, *astro-ph/0408041*

Knop et al. 2003, *ApJ*, 598, 102

Kulkarni, S. R. et al. 1999, *Nature*, 398, 389

Lamb, D. Q., & Reichart, D. E. 2000, ApJ, 536, 1

Lamb, D. Q. et al. 2004, NewA Rev., 48, 423

Liang, E. W., Dai, Z. G., & Wu, X. F. 2004, ApJ, 606, L29

Lloyd-Ronning, N. M., & Petrosian, V. 2002, ApJ, 565, 182

Lloyd-Ronning, N. M., & Ramirez-Ruiz, E. 2002, ApJ, 576, 101

MacFadyen, A.I., & Woosley, S. E. 1999, ApJ, 524, 262

Masetti, N. et al. 2000, A&A, 354, 473

Masetti, N. et al. 2002, GCN, 1330

Matheson, T. et al. 2003, ApJ, 582, L5

Panaitescu, A., & Kumar, P. 2002, ApJ, 571, 779

Perlmutter, S. et al. 1999, ApJ, 517, 565

Porciani, C. & Madau, P. 2001, ApJ, 548, 522

Press, W. H. et al 1999, *Numerical Recipes in Fortran*, Cambridge University Press, 660-664

Price, P. A. et al. 2002, ApJ, 573, 85

Price, P. A. et al. 2003, ApJ, 589, 838

Rhoads, J. E. 1999, ApJ, 525, 737

Riess, A. G. et al. 1998, AJ, 116, 1009

Riess, A. G. et al. 2004, ApJ, 607, 665

Rol, E. et al. 2003, GCN, 1981

Sakamoto, T. et al., 2004a, ApJ, 602, 875

Sakamoto, T. et al., 2004b, astro-ph/0409128

Sari, R., Piran, T., & Narayan, R. 1998, ApJ, 497, L17

Sari, R., Piran, T., & Halpern, J. P. 1999, ApJ, 519, L17

Sazonov, S. Y. et al. Nature 430, 646

Schaefer, B. E. 2003, *ApJ*, 588, 387

Schmidt, B. P. et al. 1998, *ApJ*, 507, 46

Soderberg, A. M. et al. *Nature* 430, 648

Spergel, D. N. et al. 2003, *ApJS*, 148, 175

Tegmark, M. et al. 2004, *ApJ*, 606, 702

Tiengo, A. et al. 2003, *A&A*, 409, 938

Torii, T. et al. 2002, *GCN*, 1378

Vanderspek, R. et al. 2004, preprint (astro-ph/0401311)

van den Bergh, S., & Pazder, J. 1992, *ApJ*, 390, 34

Vreeswijk, P. M. et al. 1999a, *GCN*, 324

Vreeswijk, P. M. et al. 1999b, *GCN*, 496

Vreeswijk, P. M. et al. 2003, *GCN*, 1785

Weidinger et al. 2003, *GCN*, 2215

Wu, X. F., Dai, Z. G., & Liang, E. W. 2004, *ApJ*, 615, 359

Yamazaki, R., Ioka, K., & Nakamura, T. 2004, *ApJ*, 606, L33

Zhang, B. & Mészáros, P. 2002, *ApJ*, 581, 1236

Table 1. Sample of 17 GRBs

GRB	z	$E_p^{obs}(\sigma_{E_p^{obs}})$ [KeV] ^a	$[\alpha, \beta]$ ^a	$S_\gamma(\sigma_{S_\gamma})$ [10^{-6} erg cm $^{-2}$] ^b	bandpass [KeV] ^b	$t_j(\sigma_{t_j})$ days ^c	$n(\sigma_n)$ [cm $^{-3}$] ^d	References ($z, E_p^{obs}, [\alpha, \beta], S_\gamma, t_{jet}, n$) ^e
grb970828	0.957	297.7(59.5)	-0.70, -2.07	96.0(9.6)	20-2000	2.2(0.4)	3.0(0.3)	01,18(23),23,27,01,No
grb980703	0.966	254.0(50.8)	-1.31, -2.40	22.6(2.26)	20-2000	3.4(0.5)	28.0(10.0)	02,18(23),23,27,28,28
grb990123	1.600	780.8(61.9)	-0.89, -2.45	300.0(40.0)	40-700	2.04(0.46)	3.0(0.3)	03,24,24,24,29,No
grb990510	1.6187	161.5(16.0)	-1.23, -2.70	19.0(2.0)	40-700	1.6(0.2)	0.29(0.14)	04,24,24,24,30,43
grb990705	0.843	188.8(15.2)	-1.05, -2.20	75.0(8.0)	40-700	1.0(0.2)	3.0(0.3)	05,24,24,24,31,No
grb990712	0.430	65.0(10.5)	-1.88,-2.48	6.5(0.3)	40-700	1.6(0.2)	3.0(0.3)	06,24,24,24,32,No
grb991216	1.020	317.3(63.4)	-1.23, -2.18	194.0(19.4)	20-2000	1.2(0.4)	4.7(2.8)	07,18(23),23,27,33,43
grb011211	2.140	59.2(7.6)	-0.84, -2.30	5.0(0.5)	40-700	1.50(0.02)	3.0(0.3)	08,18,18,27,34,No
grb020124	3.200	120.0(22.6)	-1.10, -2.30	6.8(0.68)	30-400	3.0(0.4)	3.0(1.0)	09,(18)25,25,25,35,No
grb020405	0.690	192.5(53.8)	0.00, -1.87	74.0(0.7)	15-2000	1.67(0.52)	3.0(0.3)	10,19,19,19,19,No
grb020813	1.250	212.0(42.0)	-1.05, -2.30	102.0(10.2)	30-400	0.43(0.06)	3.0(0.3)	11,(18)25,25,25,36,No
grb021004	2.332	79.8(30.0)	-1.01, -2.30	2.55(0.60)	2 -400	4.74(0.14)	30.0(27.0)	12,20,20,20,37,44
grb021211	1.006	46.8(5.5)	-0.805,-2.37	2.17(0.15)	30-400	1.4(0.5)	3.0(0.3)	13,26,26,26,38,No
grb030226	1.986	97.1(20.0)	-0.89, -2.30	5.61(0.65)	2 -400	1.04(0.12)	3.0(0.3)	14,20,20,20,39,No
grb030328	1.520	126.3(13.5)	-1.14, -2.09	37.0(1.40)	2 -400	0.8(0.1)	3.0(0.3)	15,20,20,20,40,No
grb030329	0.1685	67.9(2.2)	-1.26, -2.28	110.0(10.0)	30-400	0.5(0.1)	1.0(0.11)	16,22,22,22,41,45
xrf030429	2.6564	35.0(9.0)	-1.12, -2.30	0.85(0.14)	2 -400	1.77(1.0)	3.0(0.3)	17,20,20,20,42,No

| 16 |

^aThe spectral parameters fitted by the Band function. The spectra of GRB020124, GRB020813, GRB021004, GRB030226, and XRF030429 are calculated by the Band function with $\beta \sim -2.3$. For GRB011211, β is taken to be -2.3 for no available in the literature. E_p^{obs} errors are assumed to be 20% when not reported in the literature. The error of k -correction is fixed at 5%.

^bThe fluences and their errors in the observed energy band. The errors are taken as 10% when no available in the literature. The Fluences and the spectral parameters are given from the same original literature as possible. For GRB

970828, GRB 980703, GRB 991216, and GRB 011211, their the fluences and spectral parameters are not presented in the same original literature, we then choose their fluences observed in the widest energy band.

^cAfterglow break times and errors in the optical band.

^dThe circum-burst medium density and error from broadband modelling of the afterglow light curves. If no available the value of n is taken as $3 \pm 0.3 \text{ cm}^{-3}$.

^eReferences in order for z , E_p^{obs} , $[\alpha, \beta]$, S_γ , t_j , and n .

References. — (1) Djorgovski et al. 2001; (2) Djorgovski et al. 1998; (3) Hjorth 1999; (4) Vreeswijk et al. 1999a; (5) Amati et al. 2000; (6) Galama et al. 1999; (7) Vreeswijk et al. 1999b; (8) Holland et al. 2002; (9) Hjorth et al. 2003; (10) Masetti et al. 2002; (11) Price et al. 2002; (12) Matheson et al. 2003; (13) Vreeswijk et al. 2003; (14) Greiner et al. 2002; (15) Rol et al. 2003; (16) Greiner et al. 2003; (17) Weidinger et al. 2003; (18) Amati 2004; (19) Price et al. 2003; (20) Sakamoto et al. 2004b; (21) Atteia 2003; (22) Vanderspek et al. 2004; (23) Jimenez et al. 2001; (24) Amati et al. 2002; (25) Barraud et al. 2003; (26) Crew et al. 2003; (27) Bloom et al. 2003; (28) Frail et al. 2003; (29) Kulkarni et al. 1999; (30) Israel et al. 1999; (31) Masetti et al. 2000; (32) Bjornsson et al. 2001; (33) Halpern et al. 2000; (34) Jakobsson et al. 2003; (35) Torii et al. 2002; (36) Barth et al. 2003; (37) Holland et al. 2003; (38) Holland et al. 2004; (39) Klose et al. 2004; (40) Andersen et al. 2003; (41) Berger et al. 2003; (42) Jakobsson et al. 2004; (43) Panaiteescu & Kumar 2002; (44) Schaefer et al. 2003; (45) Tiengo et al. 2003

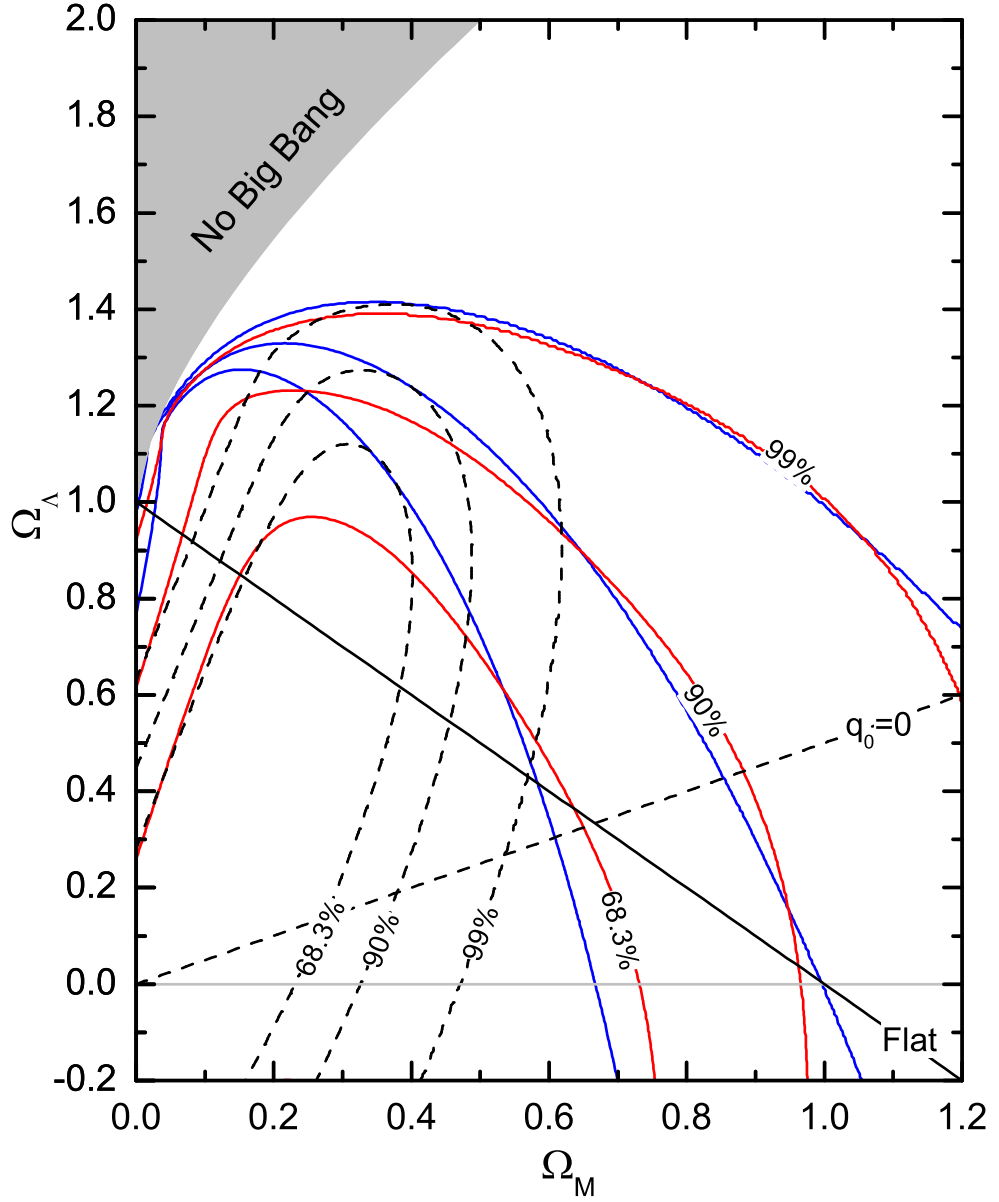


Fig. 1.— Joint confidence intervals (68.3%, 90% and 99%) for $(\Omega_M, \Omega_\Lambda)$ from the 17 GRBs with Method I (blue contours), Method II (red contours), and consideration of $a = 1.5$ and $C = 1.0$ (dashed contours). Regions representing specific cosmological scenarios are also illustrated.

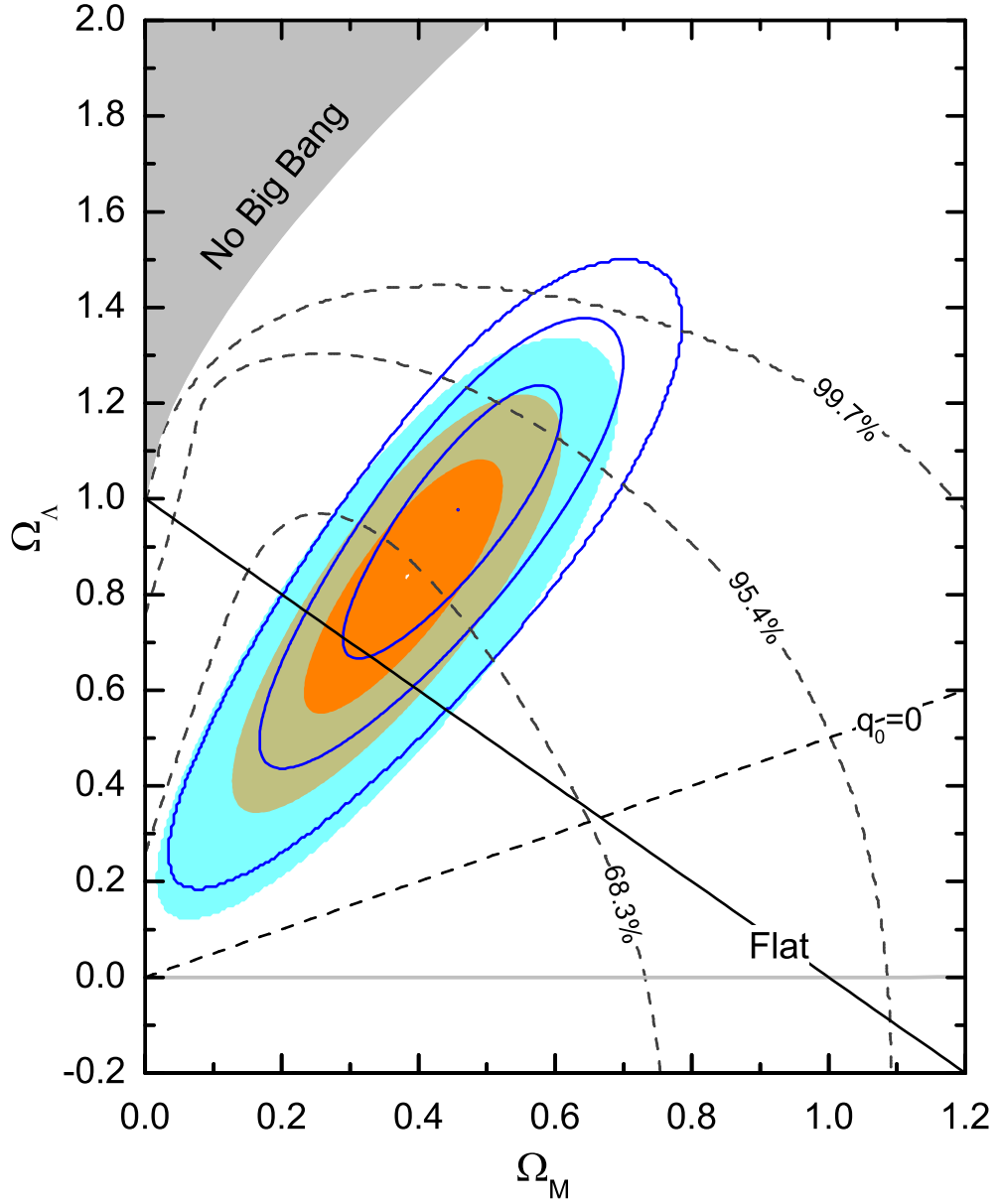


Fig. 2.— Confidence intervals (68.3%, 95.4% and 99.7%) in the $\Omega_M - \Omega_\Lambda$ plane from the 17 GRBs with Method II (dashed contours), from the SN gold sample (blue contours) and from the SN+GRB data (color regions). The upper and lower dots indicate the best-fits from the SN sample and the SN+GRB sample.

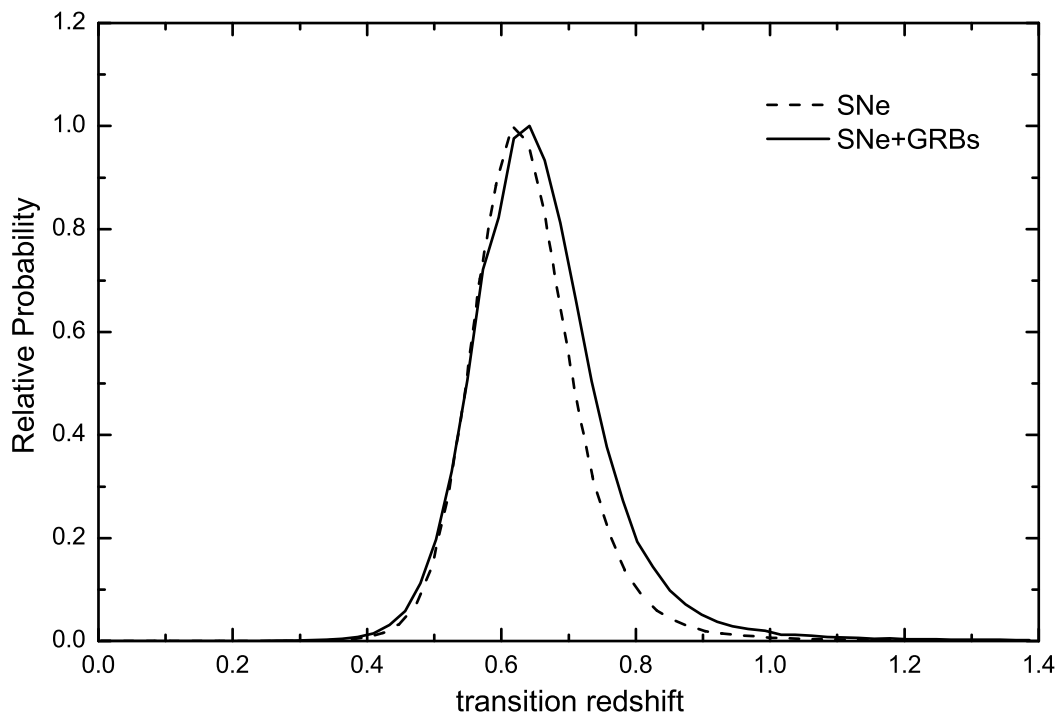


Fig. 3.— Shown are likelihood functions for the transition redshifts derived from the SN gold sample (dashed curves) and from the SN+GRB sample (solid curves), both in Λ CDM cosmology.

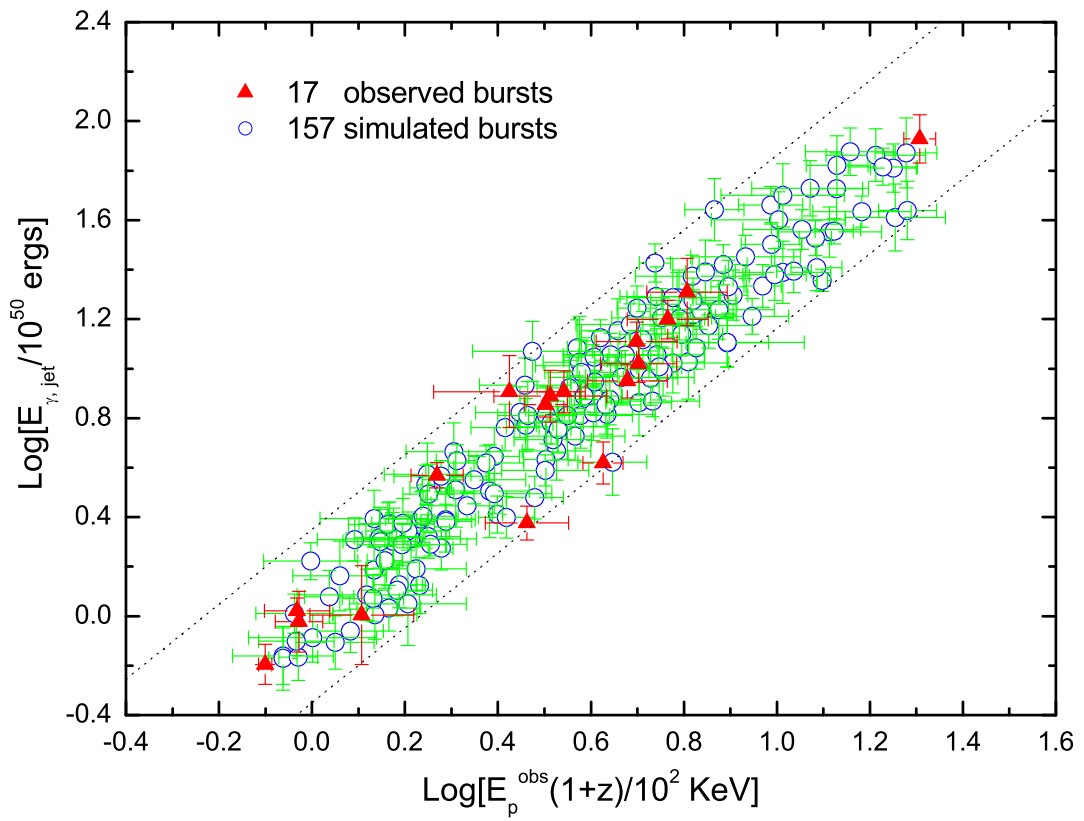


Fig. 4.— Shown are $E_{\gamma, \text{jet}}$ as a function of $E_p^{\text{obs}}(1+z)$ for the 157 simulated GRBs (open circles) and the 17 observed GRBs (filled circles).

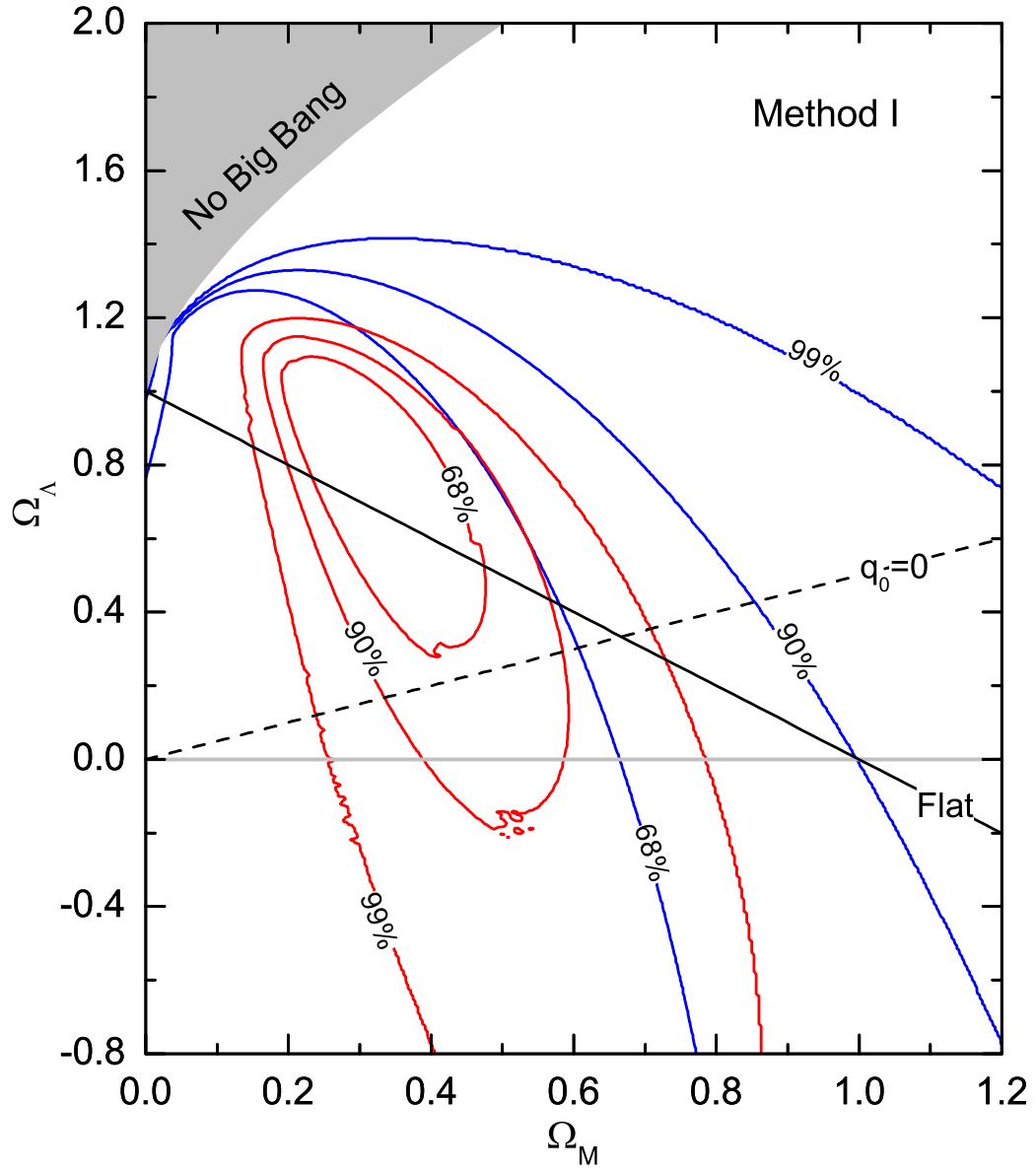


Fig. 5.— Joint confidence intervals (68%, 90% and 99%) in the Ω_M - Ω_Λ plane with Method I from the 17 observed GRBs (blue contours) and from the 157 simulated GRBs (red contours).

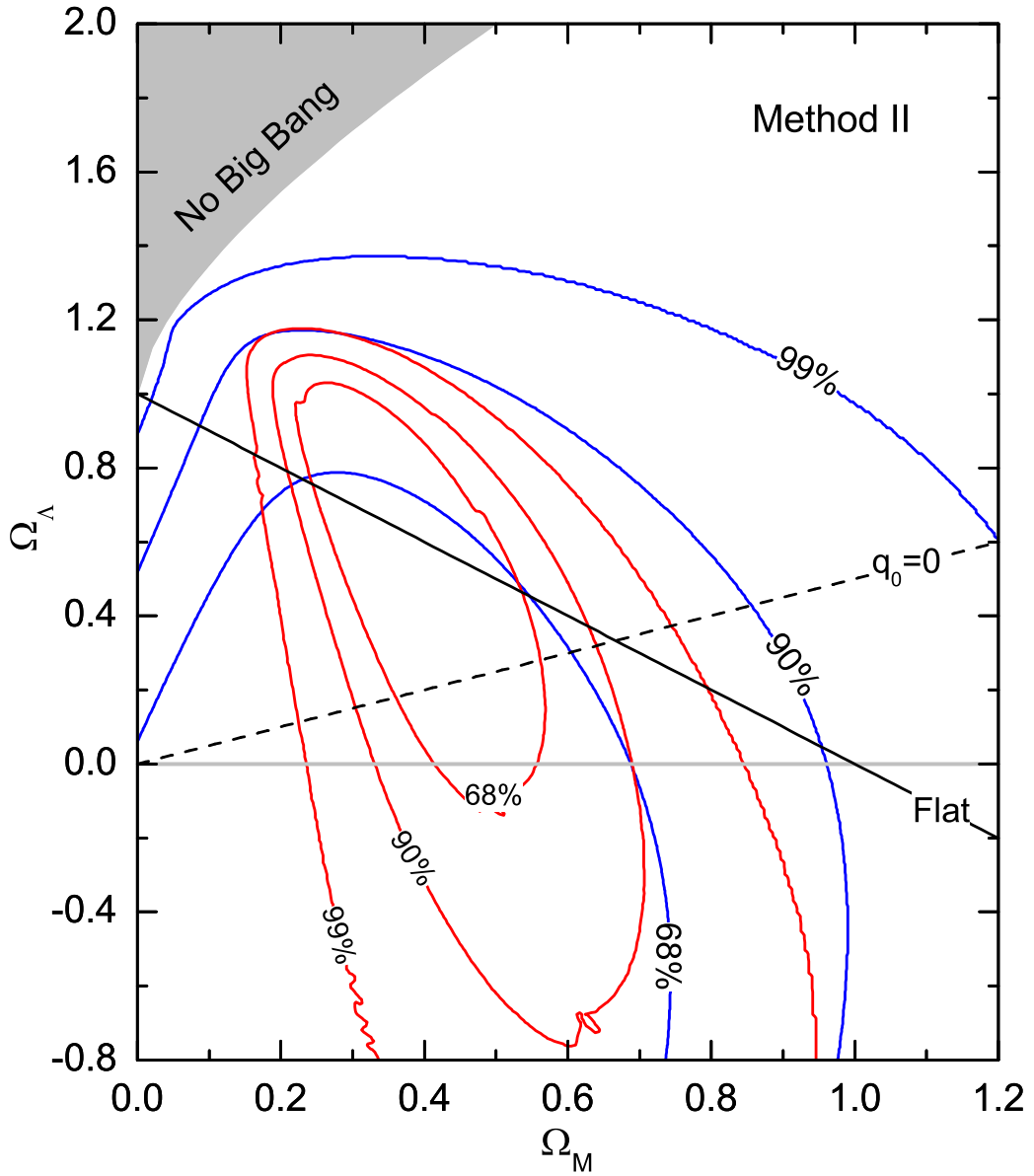


Fig. 6.— Joint confidence intervals (68%, 90% and 99%) in the Ω_M - Ω_Λ plane with Method II from the 17 observed GRBs (blue contours) and from the 157 simulated GRBs (red contours).

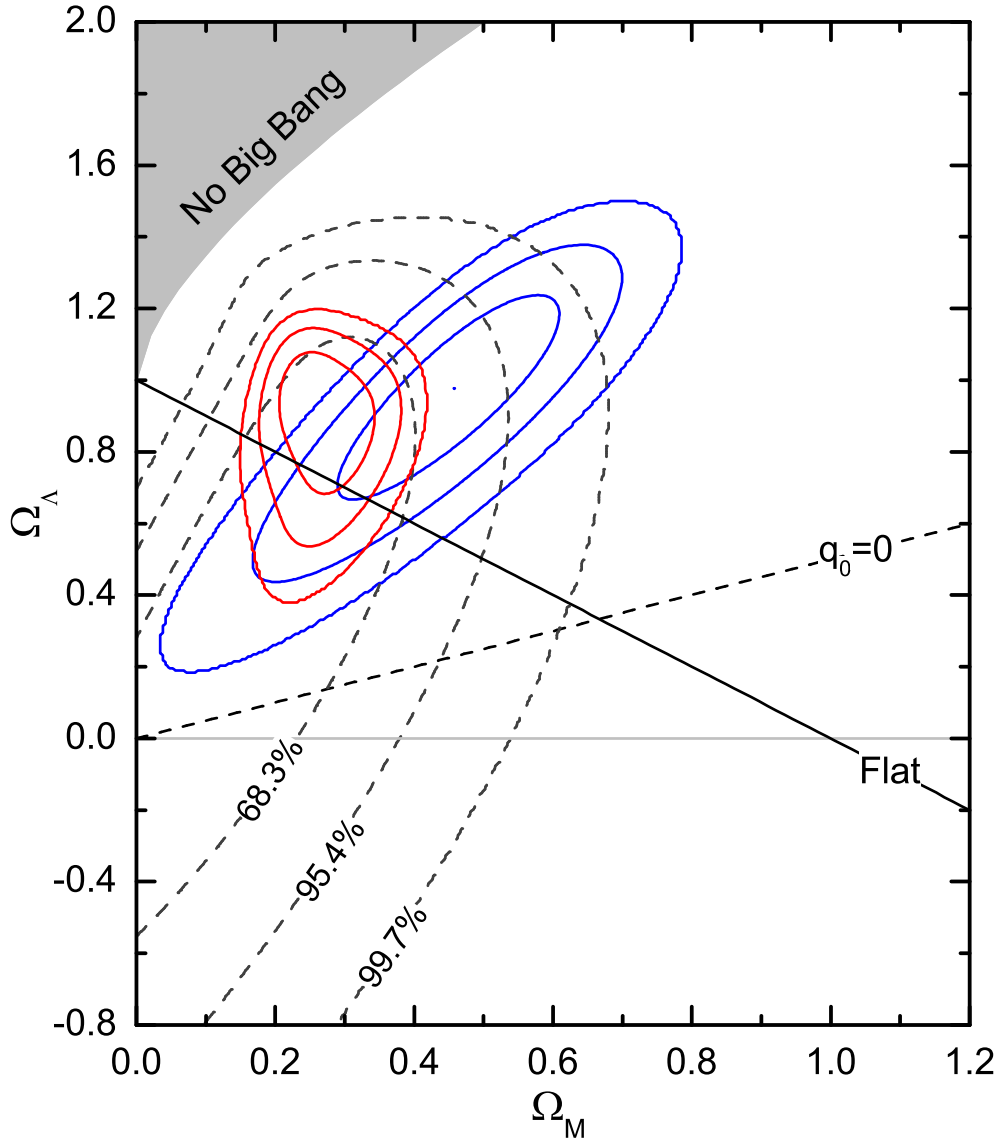


Fig. 7.— Joint confidence intervals (68.3%, 95.4% and 99.7%) in the Ω_M - Ω_Λ plane from the 157 SNe Ia (blue contours), from the 17 observed GRBs (dashed contours), and from the 157 simulated GRBs (red contours). The latter two GRB samples assume that a and C in the GGL relation are calibrated to be 1.5 and 1.0 by low- z bursts.